Journal of Magnetic Resonance **156,** 195–201 (2002)
doi:10.1006/jmre.2002.2556

Restricted Self-Diffusion of Water in a Highly Concentrated W/O Emulsion Studied Using Modulated Gradient Spin-Echo NMR

Daniel Topgaard,[1] Carin Malmborg, and Olle Söderman

Division of Physical Chemistry 1, Center for Chemistry and Chemical Engineering, Lund University, P.O. Box 124, S-221 00 Lund, Sweden

Received September 21, 2001; revised April 4, 2002

Restricted diffusion of water in a highly concentrated w/o emulsion was studied using pulsed field gradient spin echo techniques. The standard two-pulse version of this technique, suitable for analysis in the time domain, fails to investigate the short time-scale for diffusion inside a single emulsion droplet with radius 0.7 μm. With a pulse-train technique, originally introduced by Callaghan and Stepisnik, shorter time-scales are accessible. The latter approach is analyzed in the frequency domain and yields frequency dependent diffusion coefficients. Predictions for the outcome of the experiment were calculated in the time domain using the Gaussian phase distribution and the pore hopping formalism expressions for the echo attenuation. The results of these calculations were transformed to the frequency domain via a numerical inverse integral transform in order to compare with the experimental results.

Key Words: **self-diffusion; PFG SE NMR; highly concentrated emulsion; diffusion spectrum; modulated gradients.**

INTRODUCTION

Pulsed field gradient (PFG) spin echo (SE) or stimulated echo (STE) NMR is a well-established technique to noninvasively study molecular motion. The most widely used methods rely on the application of two sharp magnetic field gradient pulses which define the beginning and the end of the diffusion time (*1, 2*). The first pulse labels the position of the diffusing molecules and the second pulse reads the displacement that has occurred during the diffusion time. The observed echo intensities are conveniently analyzed in the time domain with a propagator formalism (*2, 3*). The molecular displacements can be probed over a wide range of time-scales by varying the distance between the two gradient pulses. The time-dependent diffusion coefficient and mean square displacement of a fluid imbibed in a porous matrix contain information on the porous structure, such as surface to volume ratio, pore size, and tortuosity (*4–7*). The longest diffusion time that can be observed is limited by the magnitude of the relaxation times. The shortest time accessible is set by instrumental limitations, i.e., the difficulty of applying strong and matched magnetic field gradient pulses without generating eddy currents. It is also necessary to keep the gradient pulse length much shorter than the diffusion time for the standard propagator formalism to be valid. An alternative to performing the two-pulse experiment as a function of diffusion time is to take advantage of diffraction-like effects on plots of echo intensity vs the reciprocal space vector q defined by the strength and duration of the gradient pulse (*8*). The diffraction-like features can be related to the characteristic distances in the sample, such as pore size and interpore distance.

A different approach to analyze molecular motion is to use a frequency-dependent diffusion coefficient spectrum, which is the Fourier spectrum of the translational velocity autocorrelation function (*9*). The diffusion spectrum can be probed with a train of gradient pulses where the frequency is adjusted by changing the separation between the pulses. In the case of unrestricted diffusion of small molecules the spectrum is flat for the frequencies experimentally accessible. For molecules experiencing barriers for the diffusive motion, the time between wall collisions gives rise to additional features of the diffusion spectrum. This has been demonstrated on a water-saturated packed bed of 15-μm radius polystyrene spheres (*10*). The use of a train of gradient pulses has been shown to extend the effective time-scale of NMR diffusion measurements to below 1 ms (*11*).

In this article we examine a system with micrometer-size water compartments separated by a thin oil and surfactant film, i.e., a highly concentrated w/o emulsion. With the use of two-pulse and pulse-train experiments the observational time-scales are adjusted such that both inter- and intracompartment diffusion are probed. Previous NMR studies of highly concentrated emulsions include the works of Balinov *et al.* (*12*), where the apparent water diffusion coefficient was related to the permeability of the oil and surfactant film, and Håkansson *et al.* (*13*), where methods to determine the compartment size using q-space diffusion diffractograms were developed.

THEORY

The PFG STE experiment, shown in Fig. 1, consists of a preparation interval where the first gradient pulse labels the spins with a positionally dependent phase shift and a read interval where the second gradient pulse reverses the phase shift with the

[1] To whom correspondence should be addressed. Fax: +46 46 222 44 13; E-mail: Daniel.Topgaard@fkem1.lu.se.

1090-7807/02 $35.00

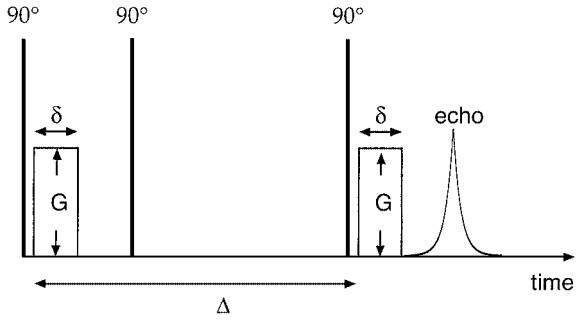

FIG. 1. The pulsed field gradient stimulated echo experiment. G and δ are the amplitude and length of the magnetic field gradient pulses. Δ is the time between the leading edges of the gradient pulses.

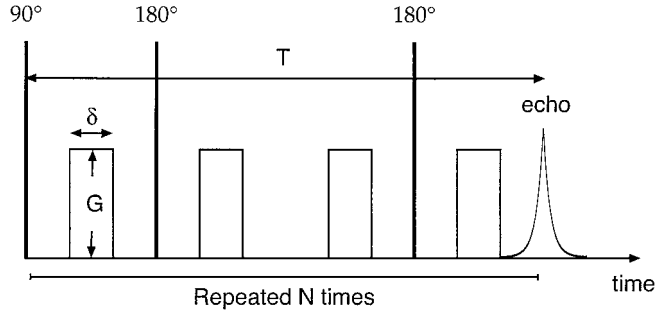

FIG. 2. The single lobe/ac modulation pulse-train sequence. The building block of the sequence is four gradient pulses and two 180° pulses in the period T. This part is repeated N times. An extra repetition without gradients is inserted before echo acquisition in order to allow for settling of eddy currents and activation of the blanking unit.

same amount for the same position in space. Diffusion between the preparation and read intervals results in an incomplete phase reversal and an attenuation of the echo. The molecular displacements taking place in the time between the gradient pulses are quantified with the propagator $P(Z, t)$ which describes the probability that a spin has the displacement Z along the gradient direction during the time t. The echo attenuation E is given by (*8*)

$$E = \int P(Z,t)\mathrm{e}^{\mathrm{i}\gamma G\delta Z}\,\mathrm{d}Z, \qquad [1]$$

where γ is the gyromagnetic ratio, G is the gradient strength, and δ is the gradient pulse length. Through a series expansion of the exponential in Eq. [1] it can be shown that the low-$G\delta$ part of the echo attenuation obeys

$$E = \mathrm{e}^{-(\gamma G\delta)^2\langle Z^2\rangle/2} \qquad [2]$$

irrespective of the actual shape of $P(Z, t)$ (as long as the average displacement $\langle Z\rangle$ is zero). The mean square displacement $\langle Z^2\rangle$ can be determined from the initial slope of a plot of $\ln E$ vs $(\gamma G\delta)^2/2$ and an apparent diffusion coefficient $D_\mathrm{t}(t)$ is defined as

$$D_\mathrm{t}(t) = \frac{\langle Z^2\rangle}{2t}, \qquad [3]$$

where $t = \Delta - \delta/3$. For free diffusion $D_\mathrm{t}(t)$ equals the true self-diffusion coefficient and is independent of t.

The diffusion spectrum $D_\omega(\omega)$ is the Fourier spectrum of the velocity auto-correlation function $\langle v(0)v(t)\rangle$

$$D_\omega(\omega) = \int_0^\infty \langle v(0)v(t)\rangle\mathrm{e}^{\mathrm{i}\omega t}\,\mathrm{d}t. \qquad [4]$$

The diffusion spectrum is sampled by $|F(\omega)|^2$ which is the frequency spectrum of the time integral of the effective gradient wave form $G(t)$

$$F(\omega) = \gamma\int_0^t\left[\int_0^{t'} G(t'')\,\mathrm{d}t''\right]\mathrm{e}^{\mathrm{i}\omega t}\,\mathrm{d}t'. \qquad [5]$$

$|F(\omega)|^2$ for the two-pulse experiment is given by (*9*)

$$|F(\omega)|^2 = \left[\gamma G\delta\Delta\frac{\sin(\omega\Delta/2)\sin(\omega\delta/2)}{(\omega\Delta/2)(\omega\delta/2)}\right]^2. \qquad [6]$$

As can be seen in Fig. 3 the sampling is dominated by the zero frequency lobe. The two-pulse experiment is thus inappropriate for frequency analysis. The single lobe/ac rectangular modulation sequence, shown in Fig. 2, has an ideal sampling function

$$|F(\omega)|^2 = \left[2\gamma G\delta\frac{\sin(N\omega T/2)\sin(\omega T/8)}{\omega\cos(\omega T/4)}\right]^2, \qquad [7]$$

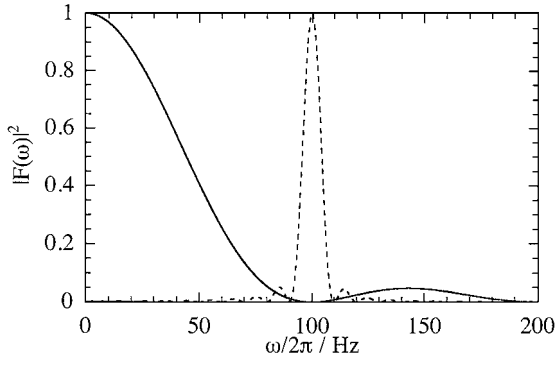

FIG. 3. $|F(\omega)|^2$ for the pulse sequences in Figs. 1 and 2. Solid line: two-pulse experiment evaluated with Eq. [6] using $\Delta = 10$ ms and $\delta = 0.5$ ms. Dashed line: pulse-train experiment evaluated with Eq. [7] using $T = 10$ ms and $N = 10$. The curves are normalized with respect to the maximum value.

where $|F(\omega)|^2$ can be considered as a delta function at $\omega = 2\pi/T$ for sufficiently high values of N. The echo attenuation for this sequence is given by (*11*)

$$E = \mathrm{e}^{-\frac{1}{2}NT(\gamma G\delta)^2 D_\omega(2\pi/T)}, \qquad [8]$$

where the symbols are defined in Fig. 2. Here the attenuation does not only depend on $G\delta$ and T, but also on N. Instead of increasing $G\delta$ when using smaller values of T it is possible to increase N to get the desired attenuation.

The mean square displacement evaluated from the diffusion spectrum is (*14*)

$$\langle Z^2\rangle = \frac{2}{\pi}\int_0^\infty D_\omega(\omega)\left[\frac{\sin(\omega t/2)}{\omega/2}\right]^2 \mathrm{d}\omega, \qquad [9]$$

which reduces to $\langle Z^2\rangle = 2Dt$ for constant $D_\omega(\omega) = D$. From Eqs. [3] and [9] a relation between the diffusion coefficient determined with the two-pulse and pulse-train methods is obtained

$$D_\mathrm{t}(t)t = \frac{1}{\pi}\int_0^\infty D_\omega(\omega)\left[\frac{\sin(\omega t/2)}{\omega/2}\right]^2 \mathrm{d}\omega, \qquad [10]$$

which can be rearranged to

$$D_\mathrm{t}(t) = \frac{t}{\pi}\int_0^\infty D_\omega(\omega)\,\mathrm{sinc}^2(\omega t/2)\,\mathrm{d}\omega. \qquad [11]$$

EXPERIMENTAL

Materials and Emulsion Preparation

Heptane of p.a. quality was purchased from Merck. The surfactant oligoethylene glycol dodecyl ether ($C_{12}EO_4$) was obtained from Nikko Chemicals, Japan. Lucas Meyer supplied soybean phosphatidylcholine with the trade name Epicuron 200. Brine was made of NaCl from Riedel–de Haen and Millipore water.

The emulsion composition was 96 wt% brine (1 wt% NaCl in Millipore water), 2.3 wt% heptane, 1.4 wt% $C_{12}EO_4$, and 0.3 wt% phosphatidylcholine. The water phase was added dropwise to the oil phase in a glass tube containing seven glass beads while shaking on a mixer. When the emulsion became viscous the shaking was done by hand. From diffusion diffractograms it could be concluded that the emulsion was stable during the time for the NMR experiments (16 h). The emulsion was aged at room temperature for 10 days before the second set of experiments was performed.

NMR Experiments

The NMR experiments were performed at 25.0°C using a Bruker DMX 200 spectrometer operating at 200.13-MHz proton resonance frequency. The 90° pulse length was 3.6 μs. The magnet was equipped with a Bruker DIFF-25 gradient probe driven by a Bruker BAFPA-40 unit. The gradient strength was calibrated from a set of PFG STE experiments using normal water, heavy water, and dodecane.

The apparent self-diffusion coefficient of water $D_\mathrm{t}(t)$ was measured with a PFG STE pulse sequence. δ was 0.5 ms and the diffusion time t was varied between 10 ms and 10 s. For each value of t the gradient was stepped up linearly to a maximum strength G_max. For each value of t, G_max was adjusted to keep $G_\mathrm{max}^2 t$ constant. G_max was 3.03 T/m at the shortest value of t.

The diffusion spectrum of water $D_\omega(\omega)$ was measured using the single lobe/ac rectangular modulation sequence with $\delta = 100$ μs, N values from 4 to 18, and T values between 2 and 100 ms. As in the two-pulse experiment the gradient strength was adjusted to keep G^2T constant. G was 9.59 T/m at the shortest value of T. To correct for transverse relaxation, each experimental echo intensity was normalized with the intensity for an equivalent experiment without gradients. To account for the imperfect rectangular shape of the rather short gradient pulses, a (frequency-independent) value of the effective $G\delta$ was estimated by adjusting the free water $D_\omega(\omega)$ between 100 and 500 Hz to the literature value. The effective $G\delta$ was found to be 5.1% larger than the nominal.

The diffusion diffractograms were recorded with the PFG STE sequence using $t = 33.8$ ms and $G_\mathrm{max} = 9.59$ T/m. δ was 3 ms for the fresh and 1.5 ms for the aged emulsion.

Noise from the gradient driver necessitated the use of a blanking unit during signal acquisition. For the two-pulse experiments the unit was opened 150 μs before and closed 150 μs after each gradient pulse. The rapid switching of gradients in the pulse-train experiment prohibited the use of the blanking unit between each gradient pulse. In this case the unit was opened before the first 90° pulse and closed before signal acquisition during the delay between the two extra 180° pulses inserted for this purpose (cf. Fig. 2).

RESULTS AND DISCUSSION

Experimental Results

In Figs. 4 and 5 we display the results of the two-pulse and pulse-train experiments. The former is reliable at values of t larger than 10 ms, while the latter works best for $\omega/2\pi$ between 70 and 500 Hz. The lower limit of the two-pulse experiment is set by mismatch between the two gradients due to the finite time required for the gradient driver to recharge after a strong gradient pulse. We note that there exists methods to overcome this problem, e.g., PGSE-MASSEY (*15*) or a train of dummy gradients before the PFG STE sequence, but none were tried here. With the pulse-train method it was possible to observe

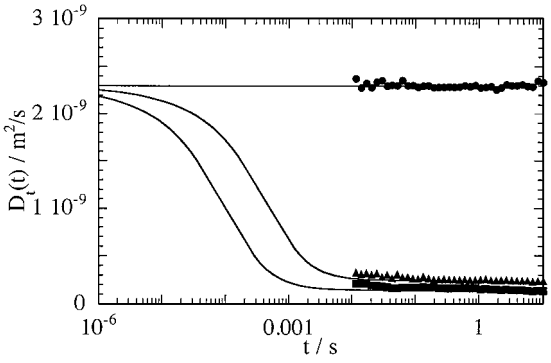

FIG. 4. The time-dependent diffusion coefficient $D_t(t)$ for free water (circles) and water confined within emulsion droplets in a highly concentrated fresh (squares) and aged (triangles) emulsion. The two lower lines are calculated using the GPD approximation for short times and the PH formalism for long times (see text for details). The upper line is the value of D for free water.

frequencies as high as 500 Hz, corresponding to a diffusion time of 2 ms. Callaghan and Stepisnik (*11*) used frequencies up to 1667 Hz. Our attempts with such high frequencies resulted in a dramatic signal loss due to eddy currents after the pulse. The residual gradients lead to a slice selection with the subsequent 180° pulse.

For the free water both methods yield a constant value for the water self-diffusion coefficient D as expected. A closer inspection of Fig. 5 reveals a slight decrease of $D_\omega(\omega)$ at the highest frequencies. This was also observed by Callaghan and Stepisnik (*11*) who attributed it to the finite rise time of the gradient leading to a slightly smaller value of $G\delta$ at higher frequencies. By using a fixed value of $D_\omega(\omega)$ for free water it is possible to calculate an effective $G\delta$ for each frequency. Since the effect is minor no such correction was made. For lower frequencies the experiment is less accurate because of the increasing influence of T_2 relaxation. This is more severe for the emulsion, not because of different T_2, but because of the order of magnitude slower long-range diffusion. Increasing the gradient strength and decreasing N is not a solution to this problem since N must be above a certain level if the sampling of $D_\omega(\omega)$ should occur at a sufficiently narrow range of frequencies (cf. Eq. [7]). The large scatter for all samples at 50 Hz we attribute to disturbances from the power supply. For the emulsions $D_t(t)$ is almost constant with the two-pulse method. At the shorter time-scales accessible with the pulse-train method a significant increase of $D_\omega(\omega)$ is observable.

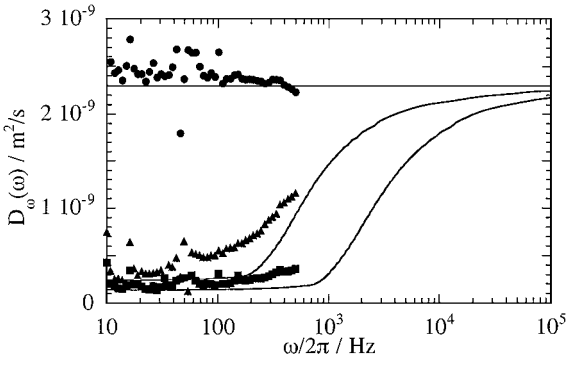

FIG. 5. The frequency-dependent diffusion coefficient $D_\omega(\omega)$ for free water (circles) and water confined within emulsion droplets in a highly concentrated fresh (squares) and aged (triangles) emulsion. The two lower lines are calculated according to the flow-scheme in Fig. 9. The upper line is the value of D for free water.

At this stage we want to relate the experimental results to the characteristic length- and time-scales for water diffusion in the emulsion. As discussed by Callaghan and Coy (*16*), the effect of restrictions for the diffusing molecules is conveniently handled with a propagator formalism. Due to the limitations of the two-pulse method we were forced to use the pulse-train method to access the shorter time-scales. We will first calculate $D_t(t)$, using a reasonable model for the structure of and water diffusion in a concentrated emulsion, and then convert it to $D_\omega(\omega)$ and compare both quantities with the experimental data.

Calculation of $D_t(t)$

For molecules diffusing in a porous medium different time-scales can be distinguished. First we consider an isolated pore with size a. At short t, $\langle Z^2\rangle^{1/2} \ll a$ and few molecules are influenced by the restrictions implying that $D_t(t) \approx D_b$, where D_b is the bulk diffusion coefficient in the absence of barriers. At intermediate t, $\langle Z^2\rangle^{1/2} \approx a$ and $D_t(t)$ is decreasing with increasing t due to the increasing number of molecules that reach the barriers. In the case of nonpermeable pore walls $\langle Z^2\rangle^{1/2}$ reaches a constant value at long t. This value is related to a and the pore shape. For spherical pores the long-time limit of $\langle Z^2\rangle^{1/2}$ is $\sqrt{2/5}a$, where a is the pore radius (*16*). In the case of permeable walls or connections between the pores, the diffusion coefficient reaches a constant value D_p reflecting the long range permeability. For discrete pores separated with a distance b there exists an intermediate diffusion time regime where the diffusing molecules sample a limited number of pores. At this time-scale diffraction-like effects can be observed in the echo-attenuation plots of intensity vs the reciprocal space vector $q = \gamma G\delta/2\pi$ (*13*). The position of the first maximum is inversely related to the distance between the center of neighboring pores b. The water droplets in a highly concentrated emulsion have a polyhedral shape but can be approximated as a sphere with radius a. Due to the limited size of the film separating the droplets we may write $b = 2a$. In Fig. 6 we display experimental echo-attenuation plots. The first maximum occurs at $q \approx 7 \cdot 10^5\ \mathrm{m}^{-1}$ for the fresh and $q \approx 3 \cdot 10^5\ \mathrm{m}^{-1}$ for the aged emulsion. Inverting these values we obtain an estimate of b, from which a is calculated. The values can be found in Table 1. To proceed we define the characteristic time for restricted diffusion inside the droplets τ_a

$$\tau_a = \frac{a^2}{2D_b} \qquad [12]$$

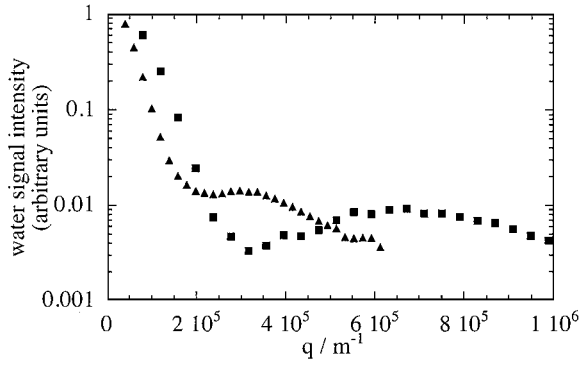

FIG. 6. Diffusion diffractogram with water signal intensity vs the reciprocal space vector q for a fresh (squares) and aged (triangles) highly concentrated emulsion. The droplet size is determined from the position of the first local maximum.

and the characteristic time for diffusion between the droplets τ_b

$$\tau_b = \frac{b^2}{2D_p}. \qquad [13]$$

For the gradient calibration we used $D_b = 2.3 \cdot 10^{-9}$ m^2/s (*17*) and from Fig. 4 we get $D_p \approx 1.4 \cdot 10^{-10}$ m^2/s for the fresh and $D_p \approx 2.4 \cdot 10^{-10}$ m^2/s for the aged emulsion. Inserting these values in Eqs. [12] and [13] gives estimates of τ_a and τ_b. The values are summarized in Table 1. In analogy with the reasoning above the regime of unrestricted diffusion is then observed at $t \ll \tau_a$ and the long-time limit is reached when $t \gg \tau_b$. Restricted diffusion inside a droplet occurs when t is on the order of 0.1 ms and the water molecules sample a limited number of droplets when t is on the order of 10 ms. Since $\tau_b \gg \tau_a$ the pore hopping (PH) formalism of Callaghan (*8*) can be used to describe the regime of t around 10 ms. With this approach it is assumed that each molecule entering a pore stays there long enough to have equal probability of being anywhere within the pore, before migrating to the next pore.

There exists expressions for $D_t(t)$ in the short-time (*4*) and long-time limit (*7*). An interpolation between the two limits has been used to describe the full range of t (*6*). For certain simple pore geometries, i.e., planar, cylindrical, and spherical geometry,

TABLE 1
Structural Parameters for the Fresh and Aged Emulsions Estimated from the Diffractogram and PFG STE Experiments

	Fresh	Aged
a/μm	0.71	1.7
b/μm	1.4	3.4
D_p/m^2/s	$1.4 \cdot 10^{-10}$	$2.4 \cdot 10^{-10}$
τ_a/ms	0.11	0.60
τ_b/ms	7.3	23

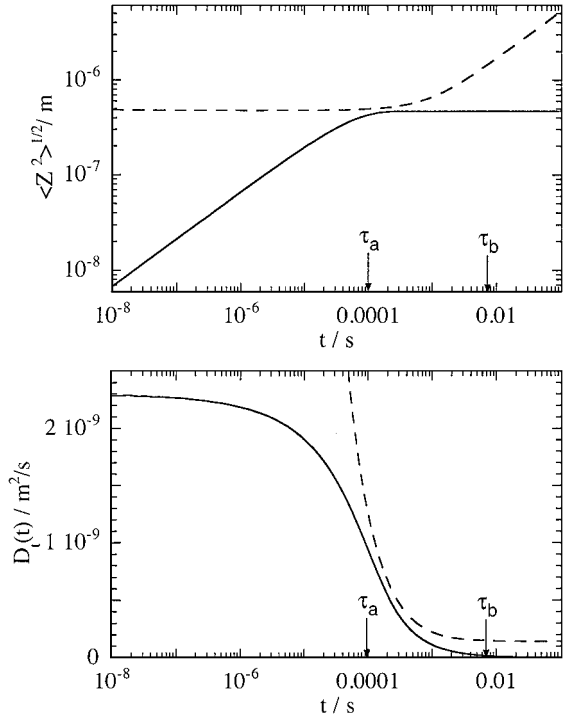

FIG. 7. Calculated $\langle Z^2 \rangle$ and $D_t(t)$ using the GPD approximation (solid line) and the PH formalism (broken line) using parameters relevant for the fresh emulsion.

there exist expressions for the echo attenuation at all values of t (*18*). The initial slope of a calculated echo-attenuation curve can be used to numerically evaluate $\langle Z^2 \rangle$ and $D_t(t)$ through Eqs. [2] and [3]. An example of such a calculation is displayed in Fig. 7 for spherical pores with radius 0.71 μm. For the calculation we used the Gaussian phase distribution (GPD) approximation for molecules diffusing in a spherical cavity with reflecting walls (*19*)

$$\ln E = -\frac{2\gamma^2 G^2}{D_b} \sum_{m=1}^{\infty} \frac{\alpha_m^{-4}}{\alpha_m^2 a^2 - 2} \times \left\{ 2\delta - \frac{2 + \exp\left[-\alpha_m^2 D_b(\Delta - \delta)\right] - 2\exp\left(-\alpha_m^2 D_b \delta\right) - 2\exp\left(-\alpha_m^2 D_b \Delta\right) + \exp\left[-\alpha_m^2 D_b(\Delta + \delta)\right]}{\alpha_m^2 D_b} \right\}, \qquad [14]$$

where α_m is the mth root of the Bessel equation $1/(\alpha a)\, J_{3/2}(\alpha a) = J_{5/2}(\alpha a)$. As can be seen in Fig. 7, $D_t(t)$ starts to drop from D_b for t orders of magnitude smaller than τ_a. When $t = \tau_a$, $D_t(t)$ is slightly less than $D_b/2$ and $\langle Z^2 \rangle^{1/2}$ reaches a constant value $\sqrt{2/5}a$. At longer t, $D_t(t)$ goes toward zero. To account for the permeability of the film separating the droplets we use the PH formalism (*16*) to calculate $D_t(t)$ in an analogous

way from the expression for a pore glass with spherical pores (*8*)

$$E = \frac{9\,[\sin(\gamma G\delta a) - \gamma G\delta a \cos(\gamma G\delta a)]^2}{(\gamma G\delta a)^6} \times \exp\left[-\frac{6D_p\Delta}{b^2}\left(1 - \frac{\sin(\gamma G\delta b)}{\gamma G\delta b}\right)\right]. \quad [15]$$

In Fig. 7 we show that at t longer than τ_b, $D_t(t)$ is equal to D_p. For shorter t, $D_t(t)$ is larger and $\langle Z^2\rangle^{1/2}$ is approaching $\sqrt{2/5}a$. The PH model is valid when the molecules have equilibrated their positions within the pore and an absolute lower limit for this is τ_a. To model our experimental system we use the isolated pore model when $t < \tau_a/2$ and the PH formalism when $t > 3\tau_a$, neglecting the region in between where neither model is valid.

Conversion of $D_t(t)$ to $D_\omega(\omega)$

From Fig. 7 it is clear that we cannot expect to observe the restricted diffusion regime with the standard PFG STE experiment, given that the shortest experimentally available diffusion time with our equipment is 10 ms. Instead, it is necessary to use the pulse-train method. A problem then arises, since most of the theory relating to restricted diffusion is handled with a propagator formalism and not with a diffusion spectrum. Equation [11] constitutes a relation between the diffusion coefficients determined with the two types of experiments. The transformation from $D_\omega(\omega)$ to $D_t(t)$ involves an integral transform with the kernel sinc^2 and the limits zero and infinity. In practice the integral is dominated by the low frequency region up to $\omega = 2\pi/t$ where the kernel has a minimum at zero ($\mathrm{sinc}^2(\pi) = 0$). Ninety percent of the kernel area is within this region. The higher frequency region still contributes a significant amount to $D_t(t)$, which makes it difficult to numerically transform experimental diffusion spectra. Theoretical expressions for the full range of $D_\omega(\omega)$ are readily transformed using numerical integration. The reverse operation is substantially more difficult. In the following section we perform the inverse integral transform by a technique similar to the ones used to make numerical inverse Laplace transforms (*20, 21*).

To evaluate $D_t(t)$ numerically, Eq. [11] must be discretized. One way to do this is by assuming that $D_\omega(\omega)$ is piecewise constant giving

$$D_t(t_i) = \sum_{j=1}^{N} A_{ij} D_\omega(\omega_j), \quad [16]$$

where

$$A_{ij} = \frac{t_i}{\pi}\,\mathrm{sinc}^2(\omega_j t_i/2)\Delta\omega_j \quad [17]$$

and $\Delta\omega_j$ is the length of the piece around ω_j. Once a proper choice of ω_j has been made the whole set of $D_t(t_i)$ can be calculated through

$$\mathbf{D}_t = \mathbf{A}\mathbf{D}_\omega, \quad [18]$$

where $\mathbf{D}_t$ is a column vector with length M and elements $D_t(t_i)$, $\mathbf{D}_\omega$ is a column vector with length N and elements $D_\omega(\omega_j)$, and $\mathbf{A}$ is a $M \times N$ matrix with elements A_{ij}. In our calculations we have typically used $N = 300$ with ω_j in a geometric series between $2\pi/t_M$ and $1000 \cdot 2\pi/t_1$. The calculation of $\mathbf{D}_t$ was described in the previous section. With the Optimization Toolbox in MATLAB the elements of $\mathbf{D}_\omega$ were varied until $\sum_i [(\mathbf{D}_t)_i - (\mathbf{A}\mathbf{D}_\omega)_i]^2$ reached a minimum. In practice it is necessary to force the solution to satisfy a series of constraints in order to get a physically reasonable result. The set of constraints used were as follows: (1) the solution is limited to the region between D_p and D_b, (2) the solution is monotonically increasing, (3) the first and final values are fixed to D_p and D_b, and (4) the solution is smoothed by a simultaneous minimization of the sum of the squares of the difference between adjacent points.

In Fig. 8a we show $D_\omega(\omega)$ obtained by the inverse integral transform of $D_t(t)$ calculated in the previous section. As can be seen in Fig. 8b the fit is more or less perfect. The appearance of $D_\omega(\omega)$ is, however, strongly dependent on the constraints used in the calculation, implying that $D_\omega(\omega)$ presented in Fig. 8a is only one in a family of solutions. Until there has been more progress in the description of $D_\omega(\omega)$ for restricted diffusion it is difficult to assess the validity of the results in Fig. 8. A flow-scheme for the calculation of $D_\omega(\omega)$ is presented in Fig. 9.

In Fig. 5 we compare the calculated $D_\omega(\omega)$ with the experimental results. Considering the approximations both in the calculation of $D_t(t)$ and in the transformation to $D_\omega(\omega)$ the

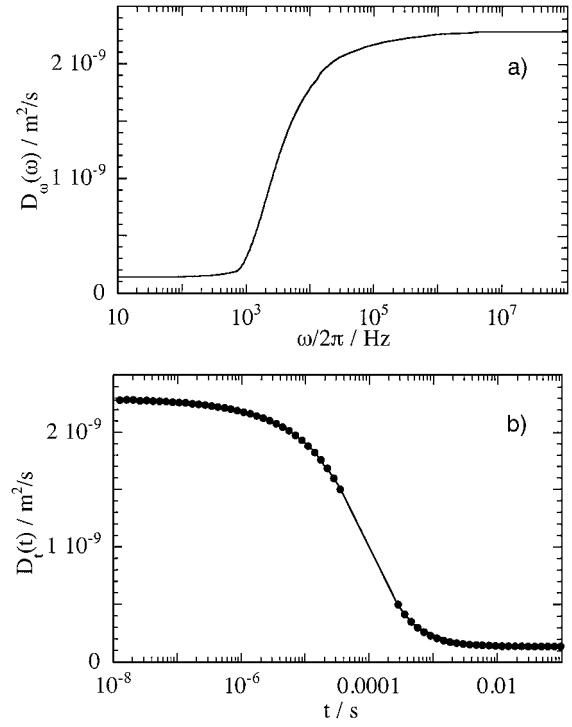

FIG. 8. (a) $D_\omega(\omega)$ calculated by solving Eq. [18] using $D_t(t)$ from Fig. 7. (b) Points, selected values of $D_t(t)$ from Fig. 7; line, fitted values.

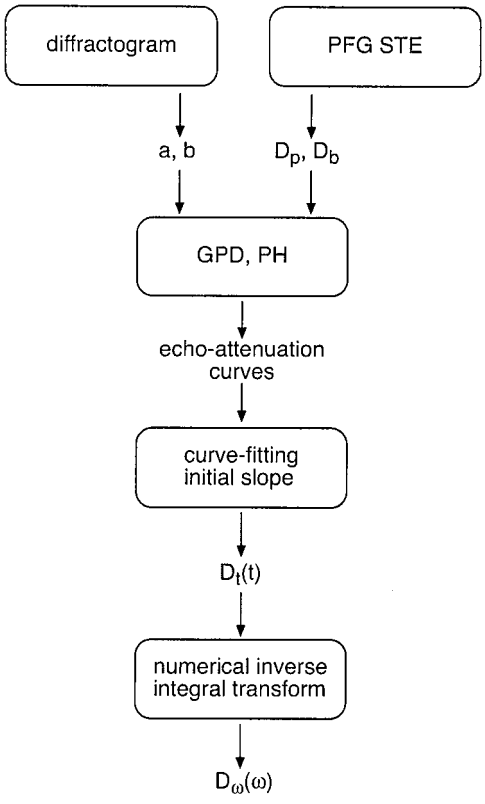

FIG. 9. Flow-scheme for the calculation of $D_\omega(\omega)$.

agreement is good. Note that there is no adjustable parameter in the calculation of $D_\omega(\omega)$. The input parameters are determined with independent NMR experiments.

To be able to observe the high frequency plateau it is necessary to use frequencies above 10 kHz, which in principle can be obtained by using the static gradients at the fringe field of a superconducting magnet (*9*). In this case the limit is not set by the time required to switch the gradient pulses. Here the problem is the signal loss due to slice selection from the strong gradients present during the RF pulses.

CONCLUSIONS

The modulated gradient technique proposed by Callaghan and Stepisnik was used to observe the regime of restricted diffusion of water inside the droplets of a highly concentrated w/o emulsion. Theoretical self-diffusion coefficients were converted from the time to the frequency domain with a numerical inverse integral transform in order to compare with the experimental results. With the modulated gradient technique it is possible to observe shorter time-scales than with the traditional PFG STE technique.

ACKNOWLEDGMENTS

This work was financially supported by the SSF Programme Colloid and Interface Technology and the Swedish Research Council.

REFERENCES

1. E. O. Stejskal and J. E. Tanner, Spin diffusion measurements: Spin echoes in the presence of a time-dependent field gradient, *J. Chem. Phys.* **42,** 288–292 (1965).
2. E. O. Stejskal, Use of spin echoes in a pulsed magnetic-field gradient to study anisotropic, restricted diffusion and flow, *J. Chem. Phys.* **43,** 3597–3603 (1965).
3. J. Kärger and W. Heink, The propagator representation of molecular transport in microporous crystallites, *J. Magn. Reson.* **51,** 1–7 (1983).
4. P. P. Mitra, P. N. Sen, L. M. Schwartz, and P. Le Doussal, Diffusion propagator as a probe of porous media, *Phys. Rev. Lett.* **68,** 3555–3558 (1992).
5. M. D. Hürlimann, K. G. Helmer, L. L. Latour, and C. H. Sotak, Restricted diffusion in sedimentary rocks. Determination of surface-area-to-volume ratio and surface relaxivity, *J. Magn. Reson. A* **111,** 169–178 (1994).
6. L. L. Latour, P. P. Mitra, R. L. Kleinberg, and C. H. Sotak, Time-dependent diffusion coefficient of fluids in porous media as a probe of surface-to-volume ratio, *J. Magn. Reson. A* **101,** 342–346 (1993).
7. L. L. Latour, R. L. Kleinberg, P. P. Mitra, and C. H. Sotak, Pore-size distributions and tortuosity in heterogeneous porous media, *J. Magn. Reson. A* **112,** 83–91 (1995).
8. P. T. Callaghan, "Principles of nuclear magnetic resonance microscopy," Oxford University Press, Oxford (1991).
9. P. T. Callaghan and J. Stepisnik, Generalized analysis of motion using magnetic field gradients, *in* "Advances in magnetic and optical resonance" (W. S. Warren, Ed.), Vol. 19, pp. 326–389, Academic Press, San Diego (1996).
10. J. Stepisnik and P. T. Callaghan, The long time tail of molecular velocity correlation in a confined fluid: observation by modulated gradient spin-echo NMR, *Physica B* **292,** 296–301 (2000).
11. P. T. Callaghan and J. Stepisnik, Frequency-domain analysis of spin motion using modulated-gradient NMR, *J. Magn. Reson. A* **117,** 118–122 (1995).
12. B. Balinov, P. Linse, and O. Söderman, Diffusion of the dispersed phase in a highly concentrated emulsion: Emulsion structure and film permeation, *J. Colloid Interface Sci.* **182,** 539–548 (1996).
13. B. Håkansson, R. Pons, and O. Söderman, Structure determination of a highly concentrated W/O emulsion using pulsed-field-gradient spin-echo nuclear magnetic resonance "diffusion diffractograms," *Langmuir* **15,** 988–991 (1999).
14. J. Stepisnik, Time-dependent self-diffusion by NMR spin-echo, *Physica B* **183,** 343–350 (1993).
15. P. T. Callaghan, PGSE-MASSEY, a sequence for overcoming phase instability in very-high-gradient spin-echo NMR, *J. Magn. Reson.* **88,** 493–500 (1990).
16. P. T. Callaghan and A. Coy, PGSE NMR and molecular translational motion in porous media *in* "Nuclear magnetic resonance probes of molecular dynamics" (R. Tycko, Ed.), pp. 489–523. Kluwer Academic, Dordrecht (1994).
17. R. Mills, Self-diffusion in normal and heavy water in the range 1–45°, *J. Phys. Chem.* **77,** 685–688 (1973).
18. P. T. Callaghan, Pulsed-gradient spin-echo NMR for planar, cylindrical and spherical pores under conditions of wall relaxation, *J. Magn. Reson. A* **113,** 53–59 (1995).
19. J. S. Murday and R. M. Cotts, Self-diffusion coefficient of liquid lithium, *J. Chem. Phys.* **48,** 4938–4945 (1968).
20. S. W. Provencher, A constrained regularization method for inverting data represented by linear algebraic or integral equations, *Comput. Phys. Comm.* **27,** 213–227 (1982).
21. K. P. Whittal and A. L. MacKay, Quantitative interpretation of NMR relaxation data, *J. Magn. Reson.* **84,** 134–152 (1989).